# Herring spawned poleward following fishery induced collective memory loss

*Aril Slotte[1], Are Salthaug[1], Sindre Vatnehol[1], Espen Johnsen[1], Erik Askov Mousing[2, 1], Åge Høines[1], Cecilie Thorsen Broms[1], Sigurvin Bjarnason[3], Eydna í Homrum[4], Øystein Skagseth[1] and Erling Kåre Stenevik[1]

*Corresponding author, aril@hi.no
[1]Institute of Marine Research (IMR), Bergen, Norway
[2]Norwegian Meteorological Institute (NMI), Oslo, Norway
[3]Marine and Freshwater Institute (MFRI), Hafnarfjörður, Iceland
[4]Faroe Marine Research Institute (FAMRI), Tórshavn, Faroe Islands

Entrainment is a process in schooling migratory fish where routes to suitable habitats are transferred from repeat spawners to recruits over generations through social learning[1]. Selective fisheries targeting older fish may therefore result in collective memory loss and disrupted migration culture[2]. The world's largest herring (*Clupea harengus*) population has traditionally migrated up to 1300 km southward from wintering areas in northern Norwegian waters to spawn at the west coast. This conservative strategy is proposed to be a trade-off between high energetic swimming costs and enhanced larval survival under improved growth conditions[3]. Here, extensive data from fisheries, scientific surveys and tagging experiments demonstrate an abrupt ~800 km poleward shift in main spawning. The new migration was established by a large cohort recruiting when the abundance of elders were critically low following age-selective fisheries. Likely the threshold of memory required for cultural transfer was not met, a situation further exacerbated by reduced spatiotemporal overlap between elders and recruits driven by migration constraints and climate change. Finally, a minority of survivors from older generations adopted the migration culture from the recruits instead of the historically opposite. This may have profound consequences for production and coastal ecology, challenging the management of migratory schooling fish.

## Main

Collective behaviour is recognized as a significant factor driving critical transitions in migrations of animals navigating dynamic environments[4, 5]. By acting collectively, they may obtain and process information better (collective learning) and established knowledge can be transferred to new uninformed group members through social interaction (social learning), both processes play a pivotal role in decision-making[6]. The accumulation of knowledge during group navigation may lead to a migratory culture at the population level[7, 8], whereas an absence of informed leaders arising from dynamics in landscape structure, mortality and recruitment can lead to disrupted migrations[9]. When cultural behaviour significantly influences fitness, it may drive selection for traits that enhance cultural learning, leading to a reciprocal coevolution of genes and culture[10].

In marine fish, the entrainment hypothesis proposes that migrations between suitable habitats develop over generations through a process of social learning between naïve recruits and experienced repeat spawners[1]. Migration shifts typically occur when numerically dominant cohorts overflow the population[11, 12]. The underlying mechanism is likely a knife-edged response in group behaviour linked to the minimum proportion of informed and determined individuals required to lead a school[13, 14]. In addition, the quality of information they hold[14], individual traits like boldness[15, 16] and the overall heterogeneity of the group[17] may play a significant role for effective leadership. Hereunder, size can be a limiting factor for social transfer of knowledge since optimal swimming speed is proportional to body length[18]. Theoretical modelling further proposes that we may fish out the collective memory of migratory schools when targeting older fish, with abrupt changes in migration culture as the potential outcome[2].

Norwegian spring spawning (NSS) herring, the world's largest herring population[19], exhibits size-dependent migrations between feeding, wintering, and spawning grounds[3, 20, 21] (Fig. 1), likely driven by a coevolution of genetics and culture[10] in response to environmental dynamics and spatiotemporal availability of its primary prey, *Calanus finmarchicus*[21–25]. Despite fluctuating population levels and changes in feeding and wintering distributions, the population has mainly spawned on the Norwegian west coast since at least 1950[20]. This conservative strategy, involving high energetic swimming costs[26], is expected to enhance larval survival under improved growth conditions[3, 24, 27, 28] during transport to Barents Sea nurseries[29]. Here they reside until ages 3-5[30], before mixing with adults feeding in the Norwegian Sea.

Our study details an abrupt and unprecedented ~800 km poleward shift in main spawning of NSS herring from Møre to Lofoten (Fig. 1a), primarily elucidated through fishery-induced collective memory loss[2]. We question whether reduced mixing between a depleted population of elders and a bursting cohort prevented effective cultural transfer and prompted the naïve recruits to establish independent migrations later adopted by a minority of older survivors. Additionally, we explore whether migration constraints[3,26] or climate change[31] triggered the abandonment of Møre or contributed to disrupted migration culture by affecting mixing between elders and recruits. Finally, we discuss cascading effects of this event on production, coastal ecosystems and management of migratory schooling fish.

## Disrupted migration linked to fishing

We have detailed the spatiotemporal dynamics in the Norwegian, Icelandic and Faroese catch distribution over the period 1995-2024 to demonstrate migrations between feeding, wintering and spawning areas (Fig.1e). During 2021-2024 the spawning migration of NSS herring significantly changed as reflected by a poleward shift in fishing pattern during the spawning season (Fig.1e, Fig. 2a), mapping of the density distribution during annual scientific acoustic-trawl surveys in February (Fig. 3b) and tag-recapture experiments (Fig. 4).

We propose that this resulted from altered demography following a bursting recruitment in 2016 (Fig 2b) combined with a depleted population of older spawners (Fig 2c) linked to age-selective fisheries (Fig 2d, e, f). The fishing pressure on adults age 5-12+ is within precautionary limits, although point estimates suggest periods with unsustainable fishing (Fig 2e) partly linked to an overestimated population in the past (Fig. 2c) and quotas being set higher than what is considered precautionary today. However, the increasing fishing pressure with age (Fig 2f) is likely the main human impact to altered demography.

After the birth of the 2016-cohort international quota negotiations among the fishing nations failed to reach agreement on the sharing of the total allowable catch, resulting in sustained overfishing of advised quotas by 40 % during 2017-2022 (Fig. 2d). Despite this, the recruitment of the 2016-cohort managed to maintain total spawner biomass just above defined precautionary levels, while the biomass of the older generations plummeted by 68%, dropping from approximately 4.0 to 1.3 million tonnes from 2019 to 2023 (Fig. 2c). By 2021 onwards, the proportion of the 2016-cohort surpassed the elders in landings and acoustic surveys (Fig. 2g) during the feeding (Extended data Figs. 1-2) and spawning (Fig. 3b) seasons.

## Why memory loss could explain the shift

We argue that under the absence of the minimum proportion of informed elders required for effective leadership[13, 14] the recruits found their own way within the population in accordance with historical observations[11, 12]. However, the actual mechanism preventing effective learning processes and transfer of migration culture evolves at the level of group formation[4, 5, 6]. To elucidate fishery induced collective memory loss as a potential explanation for the abrupt poleward shift in spawning of NSS herring we explored the spatiotemporal development in numerical dominance of the 2016-cohort at the school level. All Norwegian, Icelandic, and Faroese data on age composition derived from commercial fishing (trawl and purse seine) and research surveys (trawl) were combined to address this essential process. We defined the structure within a single sampled catch as representative of the cohort composition at the school level and presented the proportion of the 2016-cohort as quarterly distributions over the period 2017-2024 (Fig. 3a).

The observed dynamics at the school level revealed a crucial process where the elders fed and wintered to the southwest of the recruiting 2016-cohort, resulting in reduced mixing (Fig. 3a). The elders mainly entered the coast from offshore wintering areas south of Lofoten and migrated along the shelf to spawn off Møre, while the 2016-cohort migrated from the north easternmost wintering grounds to Lofoten as a first-time spawner in 2020. This pattern persisted for the 2016-cohort over 2021-2024, ultimately defining an established culture. However, it gradually extended the feeding migration westward as it grew older, predominating in schools over larger areas within the Norwegian Sea. Concurrently, the spawning distribution of the older age classes also shifted rapidly poleward to Lofoten. The distinct process where the elders adopted the spawning area of the 2016-cohort was further quantified by acoustic trawl surveys covering the distribution over 10 days in late February 2017-2024 (Fig. 3b). This snapshot of the pre-spawning situation also revealed that cohorts born after 2016 were incorporated into the new migration culture (Fig. 3b).

Support for the development of the new migration culture was strengthened at the individual fish level through tagging experiments. Over the years 2016-2023, we tagged 202155 individual herring with Passive Integrated Transponder (PIT) tags (Fig. 4a) in the north easternmost wintering area inside the fjords (Fig. 1, Fig. 4c). Here, the 2016-cohort relative to elders predominated from the winter situation (November-December) in 2020 onwards. From 2018-2024, we scanned 2.2 million tonnes for tags in landings at Norwegian and Icelandic factories with RFID (Radio Frequency Identification) antenna systems, covering the feeding, wintering, and spawning distributions (Fig. 4b). The corresponding 10716 recaptures demonstrated that tagged herring adopted western feeding distribution, offshore wintering, and southward spawning distribution towards Møre by 2020 (Fig. 4c). However, over the next years 2021-2024, when the 2016-cohort within the tagged and non-tagged population became predominant, the tagged fish stopped migrating south, aligning with the observations at the school level (Fig. 3a) and quantified acoustic abundance (Fig. 3b).

The tag data also documented straying to other populations. Between 2021 and 2024, some recaptures were linked to catches south of 62°N in target fisheries for North Sea autumn-spawning herring. Similarly, recaptures southwest of Iceland in 2021 and 2023 originated from catches of Icelandic summer spawners. Such straying may occur when a minority of NSS herring mixes with schools from other populations during the feeding season and is subsequently guided to their home grounds.

## Memory threshold preserving culture

Theoretical models suggest that even small proportions of informed individuals can significantly influence collective behaviour, with thresholds as low as 0.1 for effective leadership[13, 14]. In NSS herring, using a similar modelling framework, the probability of changing wintering areas was 50% when the proportion of informed repeat spawners fell to 0.18, and dropped below 10% if it exceeded 0.3[12]. However, our study offers new insights into these models, indicating that disrupted migration culture may occur even at higher proportions of repeat spawners. Future models must account for the fact that cohort bursts recruit into the Norwegian Sea over a period of 2-3 years[30], and that successful knowledge transfer depends heavily on the spatiotemporal overlap between recruits and elders, which could be hindered by hetereogenety[17] in terms of size dependent migration potential[3, 21].

Relatedly, since 2016 was the first large cohort in 12 years (Fig. 2b), there was a high degree of heterogeneity within the adult population. Implicit in this scenario was the necessity for the 2016-cohort to enhance its migration potential through body growth before effectively mingling with the remaining older generations, which were exploring the borderlines of their distribution[21]. By the time of full mixture in schools all over the Norwegian Sea feeding area, the 2016-cohort had already established its own migration culture (Fig 3a, b). The quality of accumulated knowledge it held at that moment[14], likely also influenced its boldness as leaders[15, 16]. Hence, being both determined and numerically dominant[2] relative to the older cohorts, it acted as a demonstrator of migration routes rather than a follower. This effect was further amplified as subsequent cohorts adopted the new migration culture (Fig. 3b).

The development of the 2002-cohort may exemplify how traditional migration culture can be preserved under normal conditions (Extended Data Figs. 3 and 4). It was also numerically dominant compared to older generations (Fig. 2b), which were rapidly depleted by age-selective fisheries (Fig. 2c, f). However, while recruiting (2005-2007, Extended Data Fig. 4a) it interacted with older fish from the start during feeding, wintering, and spawning seasons (Extended Data Fig. 3). Feeding distribution at that time and smaller age and size gap between the 2002-recruits and the dominant 1998 and 1999-cohorts (Fig. 2b, Extended Data Fig. 4a) likely facilitated greater mixing between generations. The fastest-growing individuals from the 2002-cohort were able to follow the numerically dominant elders toward the Møre spawning grounds, and as the cohort grew and became fully recruited larger fractions migrated farther south, eventually dominating throughout the spawning range (Extended Data Fig. 4b, c, d).

In such a scenario, where learning occurs gradually over a three-year recruitment period, the proportion of informed repeat spawners necessary for leadership[13, 14] could be maintained, ensuring the successful transfer of migration culture even in large cohort influxes. Additionally, this suggests that slow-growing members of a cohort can learn not only from elders but also from the faster-growing repeat spawners within their own cohort.

## Influence of migration constraints

Diverging size between the recruits and elders may hinder learning processes during the spawning migration. We propose that social transfer must be from elders or repeat spawners from same cohort with comparable migration potential. This would under the state dependent migration hypothesis be a gradual process where recruits may start to spawn in the north and follow elder fish southwards as the migration potential increases, also constrained by capacities linked to energy stored over the feeding season[3].

Originating from the north easternmost current wintering areas at 70°N, the direct migration route to the southern tip of Møre at 62°N spans approximately 1300 km along the shelf edge (Fig. 1c). We investigated whether migration constraints could account for the observed reduction in spawning migration distance of ~800 km. Time series data on body growth in terms of total length at age 7 (Fig. 2h) and initial energy stores in terms of Fulton's condition factor ($W L^{-3}$) (Fig 2i) from 1988-2023 were analysed. The data indicated that the average fish from the 2016-cohort in 2023 was shorter than 7-year-olds of some past cohorts due to density-dependent growth[30]. However, the growth was comparable to the 2002-cohort, which wintered at the same latitudes and still spawned off Møre from age 4 onwards (Fig 1e, Extended Data Figs 3-4). Moreover, there were no indications in the condition factor suggesting constraints on initial energy compared to previous periods.

During the southward spawning migration, the herring faces the same coastal currents that later transport their offspring to the north[27, 28]. To explore the aggregated effects of internal constraints and external forces for selection of spawning locations, a simple bioenergetic model was developed. The model considered both the observed body growth, condition, and spatiotemporal variability in counter current velocities along the migration route. We simulated the migration potential of an average fish from the 2016-cohort from the first fraction spawning in 2020 until full recruitment in 2023 (Fig. 5). In accordance with observations (Fig. 3) the model predicted northern spawning close to Lofoten in 2020 due to high northward velocities in combination with a small size as first-time spawner. However, subsequent simulations indicated that the cohort should have been capable of following older fish farther south in the succeeding years as it grew larger and with weaker coastal currents. Ultimately the model predicted spawning closer to Møre in 2023. These simulated dynamics offer insights into the potential natural process if the transfer of migration culture could progress under normal conditions.

## Influence of climate change

In general, marine ectotherms are more vulnerable to warming than terrestrial ones[32]. In response to global warming, marine fish tend to seek colder waters and gradually shift distributions towards the poles[31]. We explored the climate change hypothesis by fitting generalized additive models (GAMs) to 30-year long time series (1995-2024) of zooplankton data from three cross-sections and temperature data from three monitoring stations overlapping with spawning migration and larval drift of NSS herring (Extended Data Figs. 5-8). The GAM model predictions (Extended Data Figs. 5) did not show signals supporting environmental change as trigger for the abrupt poleward shift in spawning after 2020. The results rather aligned with previous studies proposing that energetic costs of migrating to Møre[26] may be traded off against enhanced larval survival[3] in warmer waters[28] with higher prey availabilities[24, 27].

In fact, NSS herring persistently spawned off Møre for two decades (Fig.1e, Fig.2a) producing large cohorts (Fig. 2b) despite warmer waters after 2000 (Extended Data Fig. 5 f, i). Relatedly, there is a lack of a discernible trend in the timing of the spring phytoplankton bloom in the Northeast Atlantic during the period of climate change[33, 34]. The primary factors driving spring bloom timing, such as the sun's zenith angle and day length, vary with latitude but not interannualy[33]. Since herring spawning is also regulated by photoperiod[35], this suggests a long-standing adaptation to the latitudinal dynamics of spring blooming[23, 34] along the Norwegian shelf and the associated production[23] and cross shelf transport[24] of *C. finmarchicus*.

We propose that ocean warming indirectly contributed to the abrupt poleward shift in spawning by affecting mixing between recruits and elders. The summer-autumn blooms in the Northeast Atlantic, which are largely unaffected by photoperiod, have been significantly delayed under the period with climate change[34, 36]. After 2005 NSS herring extended their feeding range far southwest into late autumn[21] (Fig. 1), coinciding with unexpectedly high densities of second-generation *C. finmarchicus*[25]. Warmer waters likely allowed for the emergence of two generations, which NSS herring capitalized on[21]. A consequence was delayed return migration, with wintering occurring closer to the feeding range. This shift contributed to the observed split distribution between older generations and the recruiting 2016-cohort in the Norwegian Sea (Fig1, Fig. 3a, Extended Data Figs 1-2), which may have hindered the successful transmission of traditional migration culture.

Although northern spawning may reduce production over the long term, it can still yield large cohorts. Recruitment trends of fish populations across the Northeast Atlantic show common patterns linked to environmental and ecological dynamics[37], and the occurrence of large NSS herring cohorts appears tied to specific conditions in the coastal current[38]. Our data on cyclic trends in zooplankton and the ambient temperatures experienced by adult spawners and their offspring (Extended Data Fig. 5 c, f, i) also suggest synchronized peaks along the coast during the birth years of large cohorts, such as in 2002, 2004, and 2016, with a recent promising upward trend.

## Consequences for coastal ecology

The annual spawning of NSS herring plays a crucial role in transporting large amounts of energy from spring-summer feeding in the Norwegian Sea to the Norwegian coast[39]. At Møre, hundreds of thousands of tonnes of NSS herring have spawned over small areas in just a few days[40]. Such spawning waves have proven also to be vital for predatory fish[41]. Moreover, when spawning south, hatched larvae will spread over large areas during their northward drift with coastal currents towards Barents Sea Nurseries[27, 28]. Some even end up in coastal nurseries[29] both acting as a buffer for recruitment and enriching local fjord ecology. The NSS herring spawning holds particular importance for endangered puffin colonies, where nesting sites are closely tied to historical availabilities of fish larvae[42, 43]. Over time, we may therefore witness cascade effects along the coast for species that relies on herring spawning events in the south.

## Consequences for management

Recent reviews highlight the importance of longevity conservation in animals in general[44] and in social fish specifically[45]. In fisheries age-based indicators and reference points are suggested as key tools to mitigate negative effects of truncated age structure[46], but they do not consider the threshold of memory required to preserve migration culture [12, 13, 14]. NSS herring has spawned off southern Norway for centuries interspersed with periods of absence under climate change[47], which could be explained by failed knowledge transfer due to reduced mixing between elders and recruits when long periods of recruitment failure end with a bursting cohort. Age-selective fisheries may further accelerate such natural processes by directly removing migration memory from the population.

In Pacific herring (*Clupea pallasi*), where population growth, climate change, and fishing pressure has led to the erosion of population portfolio, finer spatial scale management strategies are suggested tools[48]. Their complex metapopulation structure is proposed to emerge from two alternative strategies; either recruits home to natal habitats in fixed proportions, or they adopt migration patterns based on the abundance of experienced spawners at each spawning site[49]. If managed spatially with optimal fishing pressure under a model assuming natal homing while recruits instead just follow the older fish, model simulations predict a potential loss of 35% of all spawning sites[50].

Our study provides empirical evidence in support of such cultural erosion linked to age-selective fisheries. It complements existing theoretical frameworks, highlighting the need for further research, especially regarding the memory threshold required to preserve migration culture. Over time, through increased migration potential or population growth likely combined with an inherent genetic predisposition for favourable environments in the south, NSS herring will probably re-establish spawning at Møre. Still, to avoid such disrupted culture and periodical loss of spawning sites in schooling fish it is critically important to integrate knowledge of social learning into future management strategies.

## References (main text)

1. Chambers, M. S. Benefits to migratory fish populations of entrainment and its potential role in fisheries collapse. ICES J. Mar. Sci. 78, 36–44 (2021). https://doi.org/10.1093/icesjms/fsaa159
2. De Luca, G., Mariani, P., MacKenzie, B. R. & Marsili, M. Fishing out collective memory of migratory schools. J. R. Soc. Interface 11, 20140043 (2014). http://dx.doi.org/10.1098/rsif.2014.0043
3. Slotte, A. & Fiksen, Ø. State-dependent spawning migration in Norwegian spring spawning herring (Clupea harengus L.). J. Fish Biol. 56, 138-162 (2000). https://doi.org/10.1111/j.1095-8649.2000.tb02091.x
4. Couzin, I. D. Collective animal migration. Curr. Biol. 28, R976–R980 (2018). https://doi.org/10.1016/j.cub.2018.04.044
5. Berdahl, A. et al. Collective behavior as a driver of critical transitions in migratory populations. Mov. Ecol. 4, 18 (2016). https://doi.org/10.1186/s40462-016-0083-8
6. Aikens, E. O. et al. Viewing animal migration through a social lens. Trends Ecol. Evol. 37, 985–996 (2022). https://doi.org/10.1016/j.tree.2022.06.008
7. Berdahl, A. M. et al. Collective animal navigation and migratory culture: from theoretical models to empirical evidence. Philos. Trans. R. Soc. Lond. B Biol. Sci. 373, 20170009 (2018). https://doi.org/10.1098/rstb.2017.0009
8. Sasaki, T. & Biro, D. Cumulative culture can emerge from collective intelligence in animal groups. Nat Commun 8, 15049 (2017). https://doi.org/10.1038/ncomms15049
9. Fagan, W. F. et al. Leadership, social learning, and the maintenance (or collapse) of migratory populations. Theor. Ecol. 5, 253–264 (2012). https://doi.org/10.1007/s12080-011-0124-2
10. Whitehead, H., Laland, K.N., Rendell, L. *et al.* The reach of gene–culture coevolution in animals. Nat Commun 10, 2405 (2019). https://doi.org/10.1038/s41467-019-10293-y
11. Corten, A. D. The role of “conservatism” in herring migrations. Rev. Fish Biol. Fish. 11, 339–361 (2002). https://doi.org/10.1023/A:1021347630813
12. Huse, G., Fernö, A. & Holst, J. C. Establishment of new wintering areas in herring co-occurs with peaks in the ‘first time/repeat spawner’ ratio. Mar. Ecol. Prog. Ser. 409, 189–198 (2010). https://doi.org/10.3354/meps08620
13. Huse, G., Railsback, S. & Fernö, A. Modelling changes in migration pattern of herring: collective behaviour and numerical domination. J. Fish Biol. 60, 571-582 (2002). https://doi.org/10.1111/j.1095-8649.2002.tb01685.x
14. Couzin, I. et al. Effective leadership and decision-making in animal groups on the move. Nature 433, 513–516 (2005). https://doi.org/10.1038/nature03236

15. Kareklas, K., Elwood, R. W. & Holland, R. A. Fish learn collectively, but groups with differing personalities are slower to decide and more likely to split. Biol. Open 7, bio033613 (2018). https://doi.org/10.1242/bio.033613

16. Jolles, J. W. et al. Consistent Individual Differences Drive Collective Behavior and Group Functioning of Schooling Fish. Curr. Biol. 27, 2862-2868.e7 (2017). https://doi.org/10.1016/j.cub.2017.08.004

17. Jolles, J. W., King, A. J. & Killen, S. S. The Role of Individual Heterogeneity in Collective Animal Behaviour. Trends Ecol. Evol. 35, 278-291 (2020). https://doi.org/10.1016/j.tree.2019.11.001

18. Ware, D. M. Bioenergetics of Pelagic Fish: Theoretical Change in Swimming Speed and Ration with Body Size. J. Fish. Res. Board Can. 35, 220-228 (1978). https://doi.org/10.1139/f78-036

19. Hay, D. E. et al. Taking stock: an inventory and review of world herring stocks in 2000. In Proceedings of the 18th Lowell Wakefield Symposium: Herring Expectations For A New Millenium, Anchorage, Alaska, 23–26 February 2000. University of Alaska Sea Grant College Program, AK-SG-01-04, 381–454 (2001). https://repository.library.noaa.gov/view/noaa/38515

20. Dragesund, O., Johannessen, A. & Ulltang, Ø. Variation in migration and abundance of Norwegian spring spawning herring (Clupea harengus L.). Sarsia 82, 97-105 (1997). https://doi.org/10.1080/00364827.1997.10413643

21. Homrum, E.í. et al. Changes towards stable good somatic condition and increased gonad investment of Norwegian spring-spawning herring (Clupea harengus) after 2005 are linked to extended feeding period. Front. Mar. Sci. 9, 803171 (2022).

22. Bachiller, E. et al. Feeding ecology of Northeast Atlantic Mackerel, Norwegian spring-spawning herring and blue whiting in the Norwegian Sea. PLoS One 11, 1–25 (2016). https://doi.org/10.1371/journal.pone.0149238

23. Broms, C. & Melle, W. Seasonal development of *Calanus finmarchicus* in relation to phytoplankton bloom dynamics in the Norwegian Sea. Deep. Res. Part II Top. Stud. Oceanogr. 54, 2760–2775 (2007). https://doi.org/10.1016/j.dsr2.2007.08.021

24. Opdal, A. F. & Vikebø, F. B. Long-term stability in modelled zooplankton influx could uphold major fish spawning grounds on the Norwegian continental shelf. *Can. J. Fish. Aquat. Sci.* **73**, 189–196 (2016). https://doi.org/10.1139/cjfas-2014-0524

25. Strand, E. et al. Spatial distributions and seasonality of four Calanus species in the Northeast Atlantic. Prog. Oceanogr. 185, 102344 (2020). https://doi.org/10.1016/j.pocean.2020.102344

26. Slotte, A. Differential utilization of energy during wintering and spawning migration in Norwegian spring-spawning herring. J. Fish Biol. 55, 1233–1257 (1999). https://doi.org/10.1111/j.1095-8649.1999.tb00834.x

27. Vikebø, F. B. et al. Spatio-temporal overlap of hatching in Norwegian spring-spawning herring and the spring phytoplankton bloom at available spawning substrata. ICES J. Mar. Sci. 69, 1298–1302 (2012). https://doi.org/10.1093/icesjms/fss083

28. Vikebø, F. B. et al. Effect of hatching date, vertical distribution, and interannual variation in physical forcing on northward displacement and temperature conditions of Norwegian spring-spawning herring larvae. ICES J. Mar. Sci. 67, 1948–1956 (2010). https://doi.org/10.1093/icesjms/fsq084

29. Holst, J. C. & Slotte, A. Effects of juvenile nursery on geographic spawning distribution in Norwegian spring-spawning herring (Clupea harengus L.). ICES J. Mar. Sci. 55, 987–996 (1998). https://doi.org/10.1006/jmsc.1998.0371

30. Engelhard, G. H. & Heino, M. Maturity changes in Norwegian spring-spawning herring before, during, and after a major population collapse. Fish. Res. 66, 299–310 (2004). https://doi.org/10.1016/S0165-7836(03)00195-4

31. Dahms, C. & Killen, S. S. Temperature change effects on marine fish range shifts: A meta-analysis of ecological and methodological predictors. Global Change Biol. 29, 4459–4479 (2023). https://doi.org/10.1111/gcb.16770

32. Pinsky, M. L. et al. Greater vulnerability to warming of marine versus terrestrial ectotherms. Nature 569, 108–111 (2019). https://doi.org/10.1038/s41586-019-1132-4

33. Friedland, K. D. *et al.* The phenology of the spring phytoplankton bloom in the North Atlantic does not trend with temperature. Elem Sci Anth **12**, 1 (2024). https://doi.org/10.1525/elementa.2023.00111

34. Silva, E., Counillon, F., Brajard, J., Korosov, A., Pettersson, L. H., Samuelsen, A. & Keenlyside, N. Twenty-one years of phytoplankton bloom phenology in the Barents, Norwegian, and North seas. Front. Mar. Sci. **8**, 1626 (2021). http://dx.doi.org/10.3389/fmars.2021.746327

35. dos Santos Schmidt, T. C., Berg, F., Folkvord, A., Pires, A. M. A., Komyakova, V., Tiedemann, M. & Kjesbu, O. S. Is it possible to photoperiod manipulate spawning time in planktivorous fish? A long-term experiment on Atlantic herring. J. Exp. Mar. Biol. Ecol. **552**, 151737 (2022). http://doi.org/10.1016/j.jembe.2022.151737

36. Friedland, K. D., Record, N. R., Pendleton, D. E., Balch, W. M., Stamieszkin, K., Moisan, J. R. & Brady, D. C. Asymmetry in the rate of warming and the phenology of seasonal blooms

in the Northeast US Shelf Ecosystem. ICES J. Mar. Sci. **80**, 775–786 (2023). http://dx.doi.org/10.1093/ices

37. Zimmermann, F., Claireaux, M. & Enberg, K. Common trends in recruitment dynamics of north-east Atlantic fish stocks and their links to environment, ecology and management. Fish Fish. **20**, 518–536 (2019). https://doi.org/10.1111/faf.12360
38. Skagseth, Ø., Slotte, A., Stenevik, E. K. & Nash, R. D. M. Characteristics of the Norwegian Coastal Current during years with high recruitment of Norwegian Spring Spawning Herring (*Clupea harengus* L.). PLOS ONE **10**, e0144117 (2015). https://doi.org/10.1371/journal.pone.0144117
39. Varpe, Ø., Fiksen, Ø. & Slotte, A. Meta-ecosystems and biological energy transport from ocean to coast: the ecological importance of herring migration. Oecologia 146, 443–451 (2005). https://doi.org/10.1007/s00442-005-0219-9
40. Skaret, G. & Slotte, A. Herring sub-mesoscale dynamics through a major spawning wave: duration, abundance fluctuation, distribution and schooling. ICES J. Mar. Sci. 74, 717–727 (2016). https://doi.org/10.1093/icesjms/fsw180
41. Høines, Å. S. & Bergstad, O. A. Resource sharing among cod, haddock, saithe and pollack on a herring spawning ground. J. Fish Biol. 55, 1233–1257 (1999). https://doi.org/10.1111/j.1095-8649.1999.tb02073.x
42. Sandvik, H. et al. Modelled drift patterns of fish larvae link coastal morphology to seabird colony distribution. Nat Commun 7, 11599 (2016). https://doi.org/10.1038/ncomms11599
43. Fayet, A. L. et al. Local prey shortages drive foraging costs and breeding success in a declining seabird, the Atlantic puffin. J. Anim. Ecol. 90, 1152–1164 (2021). https://doi.org/10.1111/1365-2656.13442
44. Kopf, R. K. et al. Loss of Earth’s old, wise, and large animals. Science **387**, eado2705 (2025). https://doi.org/10.1126/science.ado2705
45. Wilson, J. A., Giske, J. & Brown, C. Overfishing social fish. Fish Fish. (2025). https://doi.org/10.1111/faf.12880
46. Griffiths, C. A. et al. Including older fish in fisheries management: A new age-based indicator and reference point for exploited fish stocks. Fish. Fish. 25, 18–37 (2024). https://doi.org/10.1111/faf.12789
47. Alheit, J. & Hagen, E. Long-term climate forcing of European herring and sardine populations. Fish. Oceanogr. 6, 130–139 (1997). https://doi.org/10.1046/j.1365-2419.1997.00035.x

48. Stier, A. C., Shelton, A. O., Samhouri, J. F., Feist, B. E. & Levin, P. S. Fishing, environment, and the erosion of a population portfolio. *Ecosphere* **11**, e03283 (2020). https://doi.org/10.1002/ecs2.3283
49. MacCall, A. D. *et al.* A heuristic model of socially learned migration behaviour exhibits distinctive spatial and reproductive dynamics. *ICES J. Mar. Sci.* **76**, 598–608 (2018). https://doi.org/10.1093/icesjms/fsy091
50. Voss, R. et al. Quantifying the benefits of spatial fisheries management – An ecological-economic optimization approach. Ecol. Model. 385, 165–172 (2018). https://doi.org/10.1016/j.ecolmodel.2018.07.012

## Figure legends

**Fig 1. Migration strategies of herring in a dynamic environment**. **a**, Study area, highlighting the poleward shift in main spawning from Møre to Lofoten. **b**, Main currents of the area. **c**, Seasonal migrations between feeding, wintering and spawning grounds during 1988-2020. Note that NSS herring spawn at hard substrates down to 250 m depth. **d**, Migration pattern during 2021-2024. These dynamics in migration patterns are also visualised empirically in **e**, The spatiotemporal dynamics in the herring fishery. Shown here is the aggregated Norwegian, Icelandic, and Faroese catch (above 80 % of total catch) within each 0.5° latitude, 1° longitude rectangle by periods seasons. Rectangles are coloured according to the scale in the bottom right panel. Note that a change in landings during feeding season from 2011 onwards reflects fishing strategies in a period with quota reductions and not availabilities.

**Fig 2. Linking distributional change to herring population dynamics**. **a**, Centre of gravity (COG) in Norwegian landings at a latitudinal scale during 15-29 February 2000-2023. **b**, Proportion of age 4 recruits in the population. Numerical dominance (above 0.5) is marked with a dotted line. **c**, Development in spawner biomass during 1988-2023. The precautionary reference point is marked with a dotted line. Trends for fish older than the 2002- and 2016-cohort are highlighted. The perception from the 2023 assessment is compared with retrospective patterns from the 1999 and 2009 assessments. **d**, Total catch where the recent overfishing relative to quota advice is highlighted. **e**, Fishing mortality (F) of adult herring (ages 5-12+ weighted with abundance and unweighted average). The precautionary reference point for F is marked with a dotted line. **f**, Exploitation pattern (F at age), where the 2016-cohort at ages 2-7 is depicted with black dots. **g**, Dynamics in the proportion of the 2016-cohort in the total international catch and three acoustic surveys: February (Spawning), spring

(IESNS) and summer (IESSNS). Numerical dominance (above 0.5) is marked with a dotted line. **h**, Somatic growth in terms of body length of at age 7 (n = 17609). **i**, Energetic status of in terms of Fultons condition factor of pre-spawning fish (n = 36501). Confidence bands for spawner biomass (**c**) and F (**e**) denotes that estimated levels with 95% probability lies within the limits, for growth (**h**) and condition (**i**) we show 95% CIs of the means of all individual fish.

**Fig 3. The abrupt poleward shift in herring spawning linked to the recruitment of the 2016-cohort. a**, Proportion of the 2016-cohort (N 2016 / N ≤ 2016) in Norwegian, Icelandic and Faroese samples from individual fishing operations in scientific surveys and commercial fisheries assumed to represent herring age structures at the school level. Trends are traced over the years 2017-2024 and seasonal migration cycles from feeding (Q2-3) and wintering (Q3-4) one year until spawning (Q1) the next. **b**, Quantification of the poleward shift in spawning through estimates of abundance within different spatial strata from acoustic trawl research surveys (see transects in grey) covering the full distribution during a ~10 days period in late February 2018-2024. Each estimate of abundance is shown as pie chart midpoints within strata, where the size of the pie is scaled to highest estimate over the study period, and split into cohorts older than 2016, the 2016-cohort and younger fish.

**Fig 4. Migration dynamics of herring tagged in the coastal wintering area. a**, Total numbers of herring tagged during 2016-2023 with Radio Frequency Identification (RFID) technology, Passive Integrated Transponder (PIT) tags. and the estimated cohort compositions. **b**, **c**, Corresponding total numbers and spatiotemporal dynamics in catch (tonnes) scanned for tags (**b**) and recaptures (**c**), over the years 2018-2024. The tagging location is marked (red box) in the map for year 2018 recaptures.

**Fig 5. Migration potential of the 2016-cohort predicted from bioenergetic simulations. a**, Predicted migration distance in 2020-2023 over a defined route of 972 km along 13 transects. **b**, Velocity of surface currents during migration in January-February exemplified by conditions in 2020. **c**, **d**, **e**, Loss in total weight (**c**), total energy (**d**) and condition factor (CF) after spawning (**e**) when migrating southwards along the 13 transects. The migration costs include the effects of interannual and spatial variability in the velocity of coastal currents. Note here that the absolute minimum level of CF at 0.6 after spawning is shown with a dotted line (**e**) to illustrate the migration constraints related to initial size and condition (**c**, **e**). When reaching this limit, they must stop and spawn (**a**) to survive for sequential spawning events. **f**, Interannual variability in upstream velocity is illustrated as the actual swimming speed required to move the set distance of 1 (b/s) along each transect.

## Methods

### Catch data

The catch data utilised in this study, while not comprehensive in representing the entire distribution of NSS herring, serves as a crucial source for understanding spatiotemporal dynamics. Our analysis integrates catch data from Norway, Iceland, and the Faroe Islands, accounting for approximately 80% of total landings spanning the years 1995 to 2023. These data are reported annually to the International Council for the Exploration of the Seas (ICES) quarterly and organized within ICES rectangles (0.5° latitude and 1° longitude)[51]. Our analyses on changes in distribution and the defined seasonal migration culture within the population were based on monthly aggregated data per ICES rectangle prepared by each nation for the study.

Furthermore, to demonstrate the long-term stability in spawning at the west coast of Norway followed by an abrupt poleward shift, we calculated the centre of gravity (COG) in the Norwegian fishery over 14-29 February, representing fish that have arrived at their designated spawning location[52]. These data were restricted to the period 2000 onwards, when the Norwegian catch data were available at the level of individual landings from the Norwegian Directorate of Fisheries (Fangstdata (seddel) koblet med fartøydata (åpne data) | Fiskeridirektoratet). The COG was calculated as the arithmetic mean of midpoint positions in statistical rectangles (system of the Norwegian directorate of fisheries, mostly 0.5° latitude and 1° longitude) weighted by the corresponding total catch within the rectangles and the specified date interval. Note that we only describe the temporal dynamics in COG on the latitudinal scale.

### Population dynamics data

Numerical dominance of recruiting cohorts in the population as well as longer term trends in spawner biomass, catch, fishing mortalities and exploitation patterns, were described based on data available from the assessment reported by the International Council for the Exploration of the Sea (ICES)[53], covering the period 1988-2023.

Note that the assessment of NNS herring has been considerably revised over this period following changes in input data and model framework. Hence, retrospective patterns in the perception of trends in spawner biomass were demonstrated by adding data from the 1999 and 2009 ICES herring assessments[54, 55].

We defined numerical dominance of a cohort as when the proportion in numbers at age 4 among age 4 and older fish was exceeding 0.5 levels. Here the 2016-cohort sticks out as the most numerically dominant one over the period 1988-2023. Our main hypothesis was that this numerical dominance led the cohort to take its own decisions, and that the elders following high fishing pressure and plummeted abundance adopted the new established migration culture. To illustrate how the 2016-cohort left its Barents Sea nurseries and recruited to the spawning population over the period 2017-2023, we presented the proportion in abundance estimates from specific acoustic trawl surveys covering the full feeding distributions in the Norwegian Sea in spring (IESNS survey) and summer (IESSNS survey) as well as the spawning season (Spawning survey) based on data from the recent assessment report[53].

Moreover, given the expected importance of mixing processes between recruits and elders during feeding in the Norwegian Sea, spatial variation in abundance were detailed as 1 nmi Nautical Area back Scattering Coefficient (NASC)[56] values along the defined transects during the IESNS and IESSNS surveys. Further details from these surveys and the methodology used is available in full survey reports attached in the annual ICES herring assessments in 2017-2023[57, 58, 59, 60, 61, 62, 53].

One parameter linked to population dynamics of specific relevance to migration potential is body growth[20, 26]. Fluctuations in growth during 1988-2023 were analysed using IMRs biological data on total body lengths (L) in cm from fully recruited 7-year-old individuals sampled during quarter 1 (n = 17609) collected in the commercial fishery and research vessel trawl hauls.

Another parameter having significant effect on spawning migration specifically is the amount of energy reserves available in this non-feeding period[26, 33]. Hence, corresponding trends in body condition were analysed with a combination of L and total weight (W) in g of individual fish, using the Fultons Condition Factor ($CF = W\ L^{-3}\ 100$)[63], to characterise the energetic status. Here we included all data from maturing fish ($L \geq 27$ cm[64]) in January (n = 36501), which should represent the initial condition of the population at the onset of spawning migration.

## Spatiotemporal cohort data

An important assumption of our study is that the effects of numerical domination for learning processes and transfer of migration culture occur at the school level. To explore the spatiotemporal development in numerical dominance of the 2016-cohort in schools linked to the abrupt poleward shift in spawning, we analysed a vast material of biological samples (n = 3226) from single trawl hauls and purse seine sets over the period 2017-2024. These were from Norwegian, Icelandic and Faroese fisheries as well as relevant surveys, including the international ecosystems surveys in the Norwegian Sea in spring (IESNS) and summer (IESSNS) and the spawning survey in February. We filtered the samples containing randomly aged individuals from the 2016-cohort and older fish (total n = 91878) assumed to represent the cohort structure within a school. The spatiotemporal dynamics of the 2016-cohort at the school level were then demonstrated by mapping the proportion of this cohort in all samples quarterly over annual migration cycles, starting during the feeding season in quarter 2 and ending during the spawning season quarter 1.

A similar analysis was conducted for the available samples (n =1748) and aged fish (n = 61616) of the 2002-cohort and older fish during the period it recruited to the spawning population 2003-2010. This comparative analysis was relevant since the 2002-cohort wintered at same latitudes as the 2016-cohort but still migrated all the way to spawn off the Norwegian west coast. To illustrate how body growth influenced the progress of southward spawning of the 2002-cohort, we first described how it gradually became numerically dominant in acoustic trawl surveys conducted during late autumn in the northern wintering areas over the years 2004-2006 according to data from the 2007 ICES assessment[65]. Secondly, we showed how these dynamics were related to growth based on IMR biological data on development in body lengths of this cohort during the wintering situation in quarter 4 over the years 2004-2006 (n = 1781). Thirdly, we demonstrated how the proportion of the cohort progressed with the distance of the spawning migrations on a latitudinal range and over the years 2005-2007 based on aged data from quarter 1 (n =8135). Finally, we addressed how these dynamics corresponded with dynamics in body lengths of the 2002-cohort (n = 2338).

While both data on fisheries and fraction of the 2016-cohort in schools served as evidence for an abrupt poleward shift in spawning of NSS herring, the main quantification of this process was derived from the Spawning surveys during 2018-2024. All details from these surveys and the methodology used is available in full survey reports attached in the annual ICES assessments in 2018-2023[58, 59, 60, 61, 62, 53], and in the 2024 IMR survey report[66]. Note that in these years the execution of the acoustic trawl surveys was directly comparable, running northwards against the migration direction covering the full distribution within the confined spawning areas over ~10 days and same dates 14-25. February using either three (2018-2020) or two vessels (2021-2024). The survey transects were specifically designed to maintain a high degree of coverage, with trawling regularly on the acoustic registrations for biological sampling and aging of ~50 specimens per haul. The same software (StoX[67]) and statistical approach was used to estimate the cohort abundance within pre-specified strata for all surveys. The poleward shift in distribution linked to the spatiotemporal development in numerical dominance of the 2016-cohort was explored by comparing the acoustic abundance relative to the aggregated abundance of older and younger fish as cake diagrams at strata midpoints in maps. Here the size of cakes was weighted to the highest acoustic abundance estimate at any strata within each survey year.

## Tag-recapture data

In the present study we also demonstrate the migration behaviour of individually tagged herring to support the observed dynamics at the population and school level. The tagging program on NSS herring using Radio Frequency Identification (RFID) technology was initiated by IMR in 2016 for assessment purposes and migration studies. All data relevant to the tagging program are open to the public through APIs[68].

During 2016-2023 herring has been tagged on annual basis over a period of three weeks in the wintering areas in fjords of northern Norway during November-January. Passive Integrated Transponder (PIT) tags, type ISO FDX-B 134,3 kHz, 3.85x23mm biocompatible glass tags are used in the experiments.

IMR rents a commercial purse sein vessel for the tagging surveys. Here herring are captured on daily basis with purse seine early in the morning and pumped gently onboard to the Refrigerated Sea Water (RSW) storage tanks though pipes with sea water. These tanks are normally used to store the catch cold until landed at a factory, but here they are specially equipped with small keeping nets for the purpose of holding the live herring until tagging. From these tanks the individual fish is dip netted and tags are injected into the abdomen. All tagged fish are transferred to a smaller storage tank and released to the sea in schools of 200 individuals. Regarding animal welfare, the tagging experiments are approved by the Norwegian Food Safety Authority (FOTS), which handles all applications to use animals in scientific experiments. During the tagging process a PC-reader system with RFID antenna is continuously recording the unique tag IDs together with the body length and other details relevant for the experiment, which frequently are synchronized with an IMR database over internet. In addition, biological samples with age and length measurements forms the basis for forward Age Length Keys (ALKs) describing age probabilities at size[69], which is used estimate numbers released by each cohort.

The PIT-tagged herring are later recaptured at Norwegian and Icelandic factories producing landings from the commercial fishery for human consumption. Here several factories are equipped with monitoring systems including RFID antennas specially designed for pipes (round antennas) or conveyor belt systems (flat antennas) detecting tagged fish during the production process. These antennas are connected to PC-reader systems that communicate directly with the IMR database providing updated information of recaptures in real time.

In addition, all relevant data from the catches scanned for PIT-tags, including vessel info, catch quantum, catch position (ICES rectangle), catch date and production time is uploaded to the database at a later stage. Finally, allocations between recaptures and catches are based on the combined info from time of recapture and the specific catch produced at that same time. In the present study we present info on the distribution and biomass of all the catches scanned for tags, as well as the distribution of recaptures from all the experiments 2016-2023.

## Bioenergetic migration model

NSS herring do not feed during spawning migration, they rely on stored reserves[26]. The energy used during the spawning migration was modelled using a simple migration model coupled with a respiration model. In the migration model, the fish follow a predetermined route defined from the observed distribution of 1 nmi NASCs during the acoustic trawl survey in 2018[58]. For each latitude increment of 0.5°, the centre of gravity was calculated, resulting in 14 locations, connected by 13 transects and with a total swimming route length of 927 km.

The southward spawning migration of NSS herring is constrained by the external forces of the coastal currents. In the migration model the interannual variations in coastal currents were included in terms mean velocities ($u$ and $v$ components) along each of the 13 transects of the migration route in 2020-2023. The velocities were obtained from the ORAS5 reanalysis produced by ECMWF provided at 0.25°x0.25° grids averaged over January-February[70]. The ocean currents on the Norwegian shelf and continental slope are largely wind driven[71]. The Norwegian Atlantic Slope Current have little vertical shear over the upper 300 m[72], where the herring migrate[58]. Hence, we assume that the surface currents are representative for the velocities herring were facing during upstream spawning migration.

Simulations were performed for observed L and W for the 2016 cohort of herring in 2020 (27.5 cm, 168 g), 2021 (29 cm, 210 g), 2022 (30 cm, 242 g) and 2023 (31.5 cm, 284 g) measured at onset of spawning migration in January. The condition was described using Fulton's Condition Factor. The dry weight (DW) was then calculated based on a water content of 68 %, and the DW was partitioned into 15 % gonads and 85 % somatic tissues with equal parts of fat and solids, typical for this time of year[26, 73]. Total initial energy was then calculated based on energy of gonads (25 kJ $g^{-1}$ DW) derived from the 68 % water content and known wet weight energy (8kJ $g^{-1}$ WW[73]), and the energy of somatic tissues using the known energy of fat (39.75 kJ $g^{-1}$ DW)[74] and solids (20.92 kJ $g^{-1}$ DW)[74].

During migration, the fish was set to swim with a net swimming speed of 1 body length (bl) $s^{-1}$ in line with observed migration speed of NSS herring between wintering and spawning areas[75] as well as cruising speed in tank experiments[76]. In addition, at each transect the swimming speed was increased proportionally to the counter current speed. Specifically, this was done by first calculating the swimming time ($t_0$) of a transect assuming no currents. Then the fish was advected for this amount of time, and the actual distance under the influence of currents calculated. Lastly, the actual swimming speed ($t_1$) was increased to account for the extra swimming distance imposed by advection ($t_1 = t_0$).

Respiration loss ($R_{O_2}; g\ O_2\ g^{-1}\ d^{-1}$) was calculated using a classical Hewett and Johnson model[77]:

$$R_{O_2} = f(W) \times f(T) \times f(SS, L)$$

Where $f(W)$ is the weight dependence on respiration, $f(T)$ is the impact of temperature on resting metabolism, and $f(SS, L)$ is the impact of active metabolism (i.e., swimming activity). The weight dependence was represented by an allometric scaling function as:

$$f(W) = \alpha \times W^{\beta}$$

Where W is the fish weight and $\alpha$ and $\beta$ are the intercept (0.0033 g O2 $g^{-1}$ $d^{-1}$) and slope (-0.227), respectively. The temperature dependence was calculated as an exponential function as:

$$f(T) = e^{\theta \times T}$$

Where T is the water temperature, set to 8°C according to results of the present study, and θ is a constant (0.0548 $°C^{-1}$) describing the impact of temperature on the resting metabolism. The impact of swimming activity was calculated as an exponential function as:

$$f(SS, L) = e^{T_o \times SS \times L}$$

Where $SS$ is the relative swimming speed, $L$ is the length of the fish and $T_o$ is a constant (0.03 $°C^{-1}$) describing the impact of swimming on the active metabolism. Finally, the specific respiration loss was converted to specific energy loss using an oxy-calorific coefficient of 15.062 J $g^{-1}$.

During the simulations energy consumption for swimming was extracted from the somatic tissue fat pool. If the fat pool was depleted, the fish would shift to using solids. Moreover, energy was transformed from somatic tissues into gonads at a rate of 0.01 $d^{-1}$ until they constituted 20 % of total DW, a typical level for pre-spawners in February[26].

The costs in terms of loss in W and total energy were predicted along the full migration route of 13 transects, although this evidently would not be feasible to survive for sequential spawning events. To predict the actual migration potential the condition factor after spawning (CF*) was also calculated between each transect by subtracting the gonad weight from the total weight. CF* was then used to assess how far the 2016-cohort would be able to swim in the years 2020-2023 before having to spawn assuming a lower threshold of CF* = 0.60. This threshold was set according to the observed 10 percentile of CF* among spent herring ≥ 27 cm analysed by IMR over the period 1935-2023 (n = 26452). We assume that by surpassing this threshold the risk of mortality would increase.

## Zooplankton biomass and temperature data

To explore if the recent abrupt poleward shift in NSS herring spawning could be linked to changes in the biotic and abiotic environment, we analysed IMRs 30-year long time series (1995-2024) of zooplankton data from WP2 net hauls at three cross-sections (Svinøy, Gimsøy and Fugløy) and temperature data from CTD casts at three monitoring stations (Bud, Eggum, Ingøy) overlapping with the period from onset of spawning migration 15th January[75] until the time when most offspring have reached metamorphosis 30th June[3].

IMRs temperature data from CTD casts at monitoring stations are open to the public https://www.imr.no/forskning/forskningsdata/stasjoner/view/initdownload with records at standard depths. We used data from depths 1, 5, 10, 20, 30, 50, 75, 100, 125, 150, 200 m in our analyses.

The zooplankton data were extracted from IMRs local data. They were collected with WP2 nets using mesh sizes 180 µm, according to the standard procedure for the surveys. The net was hauled vertically from 200 m to the surface or from the bottom whenever bottom depth was less than 200 m. The exception was stations at Fugløy cross section where standard hauls start at 100 m depth. All samples were sieved into the size fractions 180 – 1000 µm, 1000 – 2000 µm, and > 2000 µm, dried and weighted and data presented as g dry weight $m^{-2}$. In our analyses we only included the data from the smallest size fraction of zooplankton (180 – 1000 µm) as indices for the prey availability for larvae.

For each time series we fitted separate GAM models to the data. Zooplankton biomass were log-transformed before analysing the effects of sampling year and day of year:

$$\text{Log DW1000\_180} \sim \text{s(Year, }k = 17) + \text{s(DayOfYear, }k = 5)$$

For temperature we added the effect of sampling depth to the model:

$$\text{Temp} \sim \text{s(Year, }k = 17) + \text{s(DayOfYear, }k = 5) + \text{s(Depth, }k = 5)$$

We allowed number of knots $k$ for sampling year to be as high as possible without overfitting interannual fluctuations, and the same time we restricted $k$ for smoothers of day of year and depth where data were expected to follow a clear trend over season.

Since we wanted to look at trends in ambient temperatures, we ran two different models for temperature split into depth intervals and periods overlapping with adult spawning migration and incubated eggs on one side (depth = 50-200 m, day of year = 15-90)[40, 58, 75] and herring larvae from first feeding through metamorphosis on the other (depth = 1-50 m, day of year = 90-180)[3, 78, 79].

We inspected the GAM-model diagnostics and QQ-plots showed some minor tail issues, especially for ambient temperature of larvae where there were some high outliers. All models were still considered acceptable given that $R^2$ values were high (deviation explained were at same level) and all smoothers including the intercepts were significant.

Finally, based on the accepted GAM models the zooplankton and temperature (T°C) responses of sampling year, day of year and depth (only for T) were predicted at set values of covariates: year was set to 2021 to represent the poleward shift of spawning, 1st March and 150 m was used as typical time and depth of spawning[40], 1st April was considered first feeding date of larvae[78], whereas 1st May and 25 m represented time and depth of early growth larvae[79].

## Oceanographic currents in study area

In our introduction we give a schematic overview over main oceanographic currents in our study area (adopted from[80]), to demonstrate the dynamic environment herring is experiencing during it season migrations between wintering, spawning and feeding habitats.

## Data availability

Data are publicly available at https://git.imr.no/pelagic/public/paper_numeric_dominance_herring. Some are extracted from databases where data are publicly available upon request, hereunder all national biological herring data and monthly catch data aggregated ICES rectangles (0.5° latitude and 1° longitude) delivered by IMR, MFRI and FAMRI for this study. Likewise the zooplankton data and estimates of herring abundance at age by strata in StoX projects from spawning surveys were extracted from local IMR data bases, while for IESNS and IESSNS 1 nmi NASC (Nautical Area Scattering Coefficient) values along acoustic transects were extracted from Stox projects in ICES Working Group on International Pelagic Surveys (WGIPS). Other data used are publicly available for downloading, hereunder temperature data from IMRs coastal monitor stations (https://www.imr.no/forskning/forskningsdata/stasjoner/view/initdownload), current velocities along the Norwegian coast in January-February from Copernicus Marine Service Information (CMEMS) (https://doi.org/10.48670/moi-00024), individual catch data in February from The Norwegian Directorate of Fisheries (Fangstdata (seddel) koblet med fartøydata (åpne data) | Fiskeridirektoratet), and the PIT-tag data for IMRs database (https://doi.org/10.21335/NMDC-2114050995). Finally, all population level data is publicly available in ICES reports[53, 54, 55].

## Code availability

R version 4.4.2 (2024-10-31) was used for analyses and plotting included in the manuscript, and all codes are made available at https://git.imr.no/pelagic/public/paper_numeric_dominance_herring. StoX 3.6.3 was used for abundance estimation in the spawning survey, and Qgis 3.22.7 was used for mapping of these surveys and acoustic abundance estimates by strata. In addition, SAS 9.4 was used to calculate centre of gravity based on single catch data from the Norwegian Directorate of Fisheries.

## Author contributions.

AS, Are Salthaug (ASH), EJ and EKS conceived the study. AS wrote the manuscript, all authors contributed to revisions and general discussions. AS, ASH, SV and ÅH did the analyses. EAM developed the bioenergetic migration model together with AS. CTB contributed as a zooplankton expert with data. ØS contributed as oceanographic expert with data on currents. SB contributed with Icelandic PIT-tag data, catch data and biological data. EiH contributed with Faroese catch data and biological data.

## Competing interests

The authors have no competing interests.

## Ethics oversight

We have included data from PIT-tagging experiments on herring. These kind of experiments falls within the same category as laboratory experiments with animals. All our experiments have been approved by the Norwegian Food Safety Authority https://www.mattilsynet.no/en.

The survey methodologies used for the present study, including the sampling of herring and zooplankton, follows recommendations in protocols from the International Council for the Exploration of the Sea[81].

## Acknowledgements

We thank Patrizio Mariani and two anonymous reviewers for their valuable comments and contributions to improving the manuscript. We are indebted to the general contributions to all our colleagues and the overall extensive human and economical resources put into the collection of the

highly valuable empirical data used in our study. Without such time series, it would have been impossible to explore the underlying mechanisms to changed migrations in herring.

## References (methods)

51. ICES. Working Group on Widely Distributed Stocks (WGWIDE). ICES Sci. Rep. (2023). https://doi.org/10.17895/ices.pub.24025482.v1
52. Slotte, A. Effects of fish length and condition on spawning migration in Norwegian spring spawning herring (Clupea harengus L.). Sarsia 84, 111–127 (1999). https://doi.org/10.1080/00364827.1999.10420439
53. ICES. Working Group on Widely Distributed Stocks (WGWIDE). ICES Sci. Rep. (2023). https://doi.org/10.17895/ices.pub.24025482.v1
54. ICES. Report of the Northern Pelagic and Blue Whiting Fisheries Working Group (WGNPBW). ICES Expert Group Rep. (1999). https://doi.org/10.17895/ices.pub.22269352.v1
55. ICES. Report of the Working Group on Widely-Distributed Stocks (WGWIDE). ICES Expert Group Rep. (2009). https://doi.org/10.17895/ices.pub.19268609.v1
56. Maclennan, D. N. et al. A consistent approach to definitions and symbols in fisheries acoustics. ICES J. Mar. Sci. 59, 365–369 (2002). https://doi.org/10.1006/jmsc.2001.1158
57. ICES. Report of the Benchmark Workshop on Widely Distributed Stocks (WKWIDE). ICES Expert Group Rep. (2017). https://doi.org/10.17895/ices.pub.21947210.v1
58. ICES. Report of the Working Group on Widely Distributed Stocks (WGWIDE). ICES Expert Group Rep. (2018). https://doi.org/10.17895/ices.pub.5741
59. ICES. Working Group on Widely Distributed Stocks (WGWIDE). ICES Sci. Rep. (2019). https://doi.org/10.17895/ices.pub.5574
60. ICES. Working Group on Widely Distributed Stocks (WGWIDE). ICES Sci. Rep. (2020). https://doi.org/10.17895/ices.pub.7475
61. ICES. Working Group on Widely Distributed Stocks (WGWIDE). ICES Sci. Rep. (2021). https://doi.org/10.17895/ices.pub.8298
62. ICES. Working Group on Widely Distributed Stocks. ICES Sci. Rep. (2022). https://doi.org/10.17895/ices.pub.21088804.v1
63. Ricker, W. E. Computation and interpretation of biological statistics of fish populations. Bull. - Fish. Res. Board Can. 191, 1–382 (1975). https://publications.gc.ca/site/eng/480738/publication.html

64. Slotte, A., Johannessen, A. & Kjesbu, O. S. Effects of fish size on spawning time in Norwegian spring-spawning herring. J. Fish Biol. 56, 295–310 (2000). https://doi.org/10.1111/j.1095-8649.2000.tb02107.x

65. ICES. Report of the Northern Pelagic and Blue Whiting Fisheries Working Group (WGNPBW). ICES Expert Group Rep. (2007). https://doi.org/10.17895/ices.pub.19280210.v1

66. Salthaug, A. & Stenevik, E. K. Distribution and abundance of Norwegian spring spawning herring during the spawning season in 2024. IMR cruise report nr. 8 2024 (2024). https://www.hi.no/hi/nettrapporter/toktrapport-en-2024-8

67. Johnsen, E. et al. StoX: An open-source software for marine survey analyses. Methods Ecol Evol 10, 1523–1528 (2019). https://doi.org/10.1111/2041-210X.13250

68. Slotte, A. et al. PIT-tag time series for use in stock assessment and migration studies of North East Atlantic mackerel (Scomber Scombrus) and Norwegian spring spawning herring (Clupea harengus). https://doi.org/10.21335/NMDC-2114050995

69. Ailloud, L. E. & Hoenig, J. M. A general theory of age-length keys: combining the forward and inverse keys to estimate age composition from incomplete data. ICES J. Mar. Sci. 76, 1515–1523 (2019). https://doi.org/10.1093/icesjms/fsz072

70. E.U. Copernicus Marine Service Information (CMEMS). Global Ocean Ensemble Physics Reanalysis. https://doi.org/10.48670/moi-00024 (Accessed on 12-Jan-2025)

71. Skagseth, Ø., Orvik, K. A. & Furevik, T. Coherent variability of the Norwegian Atlantic Slope Current derived from TOPEX/ERS altimeter data. Geophys. Res. Lett. 31, L14304 (2004). https://doi.org/10.1029/2004GL020057

72. Orvik, K. A., Skagseth, Ø. & Mork, M. Atlantic Inflow to the Nordic Seas. Current structure and volume fluxes from moored current meters, VM-ADCP and SeaSoar-CTD observations, 1995-1999. Deep-Sea Res. 48, 937–957 (2001). https://doi.org/10.1016/S0967-0637(00)00038-8

73. McGurk, M. D. et al. Condition indices, energy density and water and lipid content of Atlantic herring (Clupea harengus) of southeastern Newfoundland. Can. Tech. Rep. Fish. Aquat. Sci. 958, 41 pp. (1980). https://publications.gc.ca/site/fra/452192/publication.html

74. Beamish, F. W. H., Niimi, A. J. & Lett, P. F. K. Bioenergetics of teleost fishes. In Proc. Int. Conf. Comp. Physiol.—Func. Aspects Struct. Mater. (Bolis, L., Maddrell, S. H. P. & Schmidt-Neilson, K., eds), pp. 187–209 (North Holland Publishing Company, 1975).

75. Slotte, A. Effects of fish length and condition on spawning migration in Norwegian spring spawning herring (Clupea harengus L.). Sarsia 84(2), 111–127 (1999). https://doi.org/10.1080/00364827.1999.10420439
76. He, P. & Wardle, C. Endurance at intermediate swimming speeds of Atlantic mackerel, Scomber scombrus L., herring, Clupea harengus L., and saithe, Pollachius virens L. J. Fish Biol. 33, 255–266 (1988). https://doi.org/10.1111/j.1095-8649.1988.tb05468.x
77. Hewett, S. W. & Johnson, B. L. Fish bioenergetics model 2: an upgrade of a generalized bioenergetics model of fish growth for microcomputers. University of Wisconsin, Sea Grant Institute, Technical Report WIS-SG92-250, Madison (1992). https://repository.library.noaa.gov/view/noaa/35468
78. Husebø, Å., Stenevik, E. K., Slotte, A., Fossum, P., Salthaug, A., Vikebø, F., Aanes, S. & Folkvord, A. Effects of hatching time on year-class strength in Norwegian spring-spawning herring (*Clupea harengus*). ICES J. Mar. Sci. **66**, 1710–1717 (2009). https://doi.org/10.1093/icesjms/fsp150.
79. Ferreira, A. S. de A., Stenevik, E. K., Vollset, K. W., Korneliussen, R. & Folkvord, A. Vertical migration of Norwegian spring-spawning herring larvae in relation to predator and prey distribution. Mar. Biol. Res. **8**, 605–614 (2012). https://doi.org/10.1080/17451000.2011.653370
80. Drinkwater, K. F., Sundby, S. & Wiebe, P. H. Exploring the hydrography of the boreal/arctic domains of North Atlantic seas: results from the 2013 BASIN survey. Deep-Sea Res. Part II Top. Stud. Oceanogr. **180**, 104880 (2020). https://doi.org/10.1016/j.dsr2.2020.104880
81. ICES. 2025. ICES Survey protocols - Manual for International Pelagic Surveys, coordinated by ICES Working Group of International Pelagic Surveys (WGIPS). ICES Techniques in Marine Environmental Sciences Vol. 71. 227 pp. https://doi.org/10.17895/ices.pub.28269671

## Extended Data Figure legends

**Extended data Fig. 1. Distribution and acoustic densities of NSS herring during the early feeding season.** Shown are 1 nmi NASC (Nautical Area Scattering Coefficient) values along acoustic transects from the international survey IESNS running from late April to early June in the Norwegian Sea 2017-2023. NASC values are scaled linearly to the highest value over the time series; 19516 in 2023.

**Extended data Fig. 2. Distribution and acoustic densities of NSS herring during the late feeding season.** Shown are 1 nmi NASC (Nautical Area Scattering Coefficient) values along acoustic transects from the international survey IESSNS running from start of July to early August in the

Norwegian Sea 2017-2023. NASC values are scaled linearly to the highest value over the time series, 42825 in 2020.

**Extended data Fig. 3**. **Spatiotemporal dynamics in proportion of the 2002-cohort in schools**. Shown is the proportion of 2002-cohort (P 2002 / P ≤ 2002) in Norwegian, Icelandic and Faroese samples from individual fishing operations in scientific surveys and commercial fisheries. Trends are traced over the years 2003-2010 and seasonal migration cycles from feeding (Q2-3) and wintering (Q3-4) one year until spawning (Q1) next year.

**Extended Data Fig. 4**. **The recruitment of the 2002-cohort to the spawning population**. **a**, Cohort abundance estimated during IMRs acoustic trawl surveys in the northeastern wintering areas in November 2004-2006. **b**, Length distribution of the 2002 cohort during quarter 4 in 2004-2006. **c,** The proportion of the 2002-cohort relative to older fish on a latitudinal range during quarter 1 2005-2007. **d**, Latitudinal differences in mean body length with 95% CIs of the 2002-cohort during the quarter 1 in 2005-2007 (n = 2338). Note that **b**, **c** and **d** is based on all biological data collected from acoustic trawl surveys and commercial fishery by IMR.

**Extended Data Fig 5. Spatiotemporal dynamics in zooplankton and temperatures at the Norwegian shelf**. **a**, zooplankton biomass time series (1000-180 µm) were from cross sections Svinøy (blue), Gimsøy (green) and Ingøy (red) whereas temperature time series were from Bud (blue), Eggum (green) and Ingøy (red) monitoring stations. b, c, d, e, f, g, h, i, Predictions from GAM models with 95% CIs fitted to 30 years of data (see Extended Data Figs 6-8). **b**, **c**, Development in zooplankton biomass: **b**, over day of year in 2021 and **c**, over years at first larval feeding 1st April. **d**, **e**, **f**, Trends in temperature during spawning migration: **d**, with depth when spawning 1st March in 2021, **e**, over day of year when spawning at 150 m depth in 2021, and **f**, over years when spawning at 150 m depth on 1st March. **g**, **h**, **i**, Trends in temperature during the larval period: **g**, with depth 1st May in 2021, **h**, over day of year at 25 m depth in 2021 and **i**, over at 1st May and 25 m depth.

**Extended Data Fig. 6**. **GAM-model diagnostics of zooplankton biomass at the Norwegian shelf**. The log dry weigh (g $m^{-2}$) of the smallest size group (1000-180 µm) relevant for herring larvae was recorded using WP2 nets at three cross sections south to north (Svinøy, Gimsøy and Fugløy) (Extended Data Fig.5a), and stations included in the analyses were those located on shelf (depth <500 m) overlapping with herring larval dispersal. We analysed data from a 30-year period (1995-2024), with focus on the season 15 January through June to representing both the spawning migration of adult fish along the coast, and the following northward larval drift period through metamorphosis. A GAM model was fitted separately to data from each of the three cross sections: DW1000_180 ~ s(Year, k = 17) + s(DayOfYear, k = 5). All three models, Svinøy (n = 457, $R^2 = 0.717$, $p < 0.001$), Gimsøy ($n = 382$, $R^2 = 0.831$, $p < 0.001$) and Fugløy ($n = 546$, $R^2 = 0.678$, $p < 0.001$) as well as their intercepts and smoothers (DayOfYear, Year, $p < 0.001$) were highly significant. Output: **a**, Distribution of raw data over day of year for the three models. **b**, **c**, Partial effects of smoother terms at their covariate means with 95% CIs. **d**, **e**, Model diagnostic plots showing **d**, fitted values versus residuals and **e**, QQ plots.

**Extended Data Fig. 7**. **GAM-model diagnostics of ambient temperatures during spawning migration**. Temperature data were analysed from three monitoring stations (Bud, Eggum and Ingøy) located at different latitudes along the Norwegian shelf (Extended Data Fig.5a). Data were collected over a 30-year period (1995-2024) from 15 January through March at depths 50-200 m, representing water masses experienced by adult herring on spawning migration and their incubated eggs until peak hatching. A GAM model was fitted separately to data from each of the three monitoring stations: Temp ~ s(Year, k = 17) + s(DayOfYear, k = 5) + s(Depth, k = 5). All three models, Bud ($n = 642$, $R^2 = 0.743$, $p < 0.001$), Eggum ($n = 1162$, $R^2 = 0.720$, $p < 0.001$) and Ingøy ($N = 1032$, $R^2 = 0.589$, $p < 0.001$) as well as their intercepts and smoothers (DayOfYear, Depth, Year, $p < 0.001$) were highly significant. Output: **a**, Distribution of raw data over day of year for the three models. **b**, **c**, **d** Partial effects of smoother terms at their covariate means with 95% CIs. **d**, **e**, Model diagnostic plots showing **d**, fitted values versus residuals and **e**, QQ plots.

**Extended Data Fig. 8**. **GAM-model diagnostics of ambient temperatures during larval stage**. Temperature data were analysed from three monitoring stations (Bud, Eggum and Ingøy) located at different latitudes along the Norwegian shelf (Extended Data Fig.5a). Data were collected over a 30-year period (1995-2024) from 1.April through June at depths 1-50 m, representing water masses experienced by herring larvae from peak hatching through metamorphosis. A GAM model was fitted separately to data from each of the three monitoring stations: Temp ~ s(Year, k = 17) + s(DayOfYear, k = 5) + s(Depth, k = 5). All three models, Bud ($n = 869$, $R^2 = 0.773$, $p < 0.001$), Eggum ($n = 1583$, $R^2 = 0.847$, $p < 0.001$) and Ingøy ($n = 1260$, $R^2 = 0.813$, $p < 0.001$) as well as their intercepts and smoothers (DayOfYear, Depth, Year, $p < 0.001$) were highly significant, with one exception of $p = 0.001$ for smoother Depth at station Fugløy. Output: **a**, Distribution of raw data over day of year for the three models. **b**, **c**, **d** Partial effects of smoother terms at their covariate means with 95% CIs. **d**, **e**, Model diagnostic plots showing **d**, fitted values versus residuals and **e**, QQ plots.

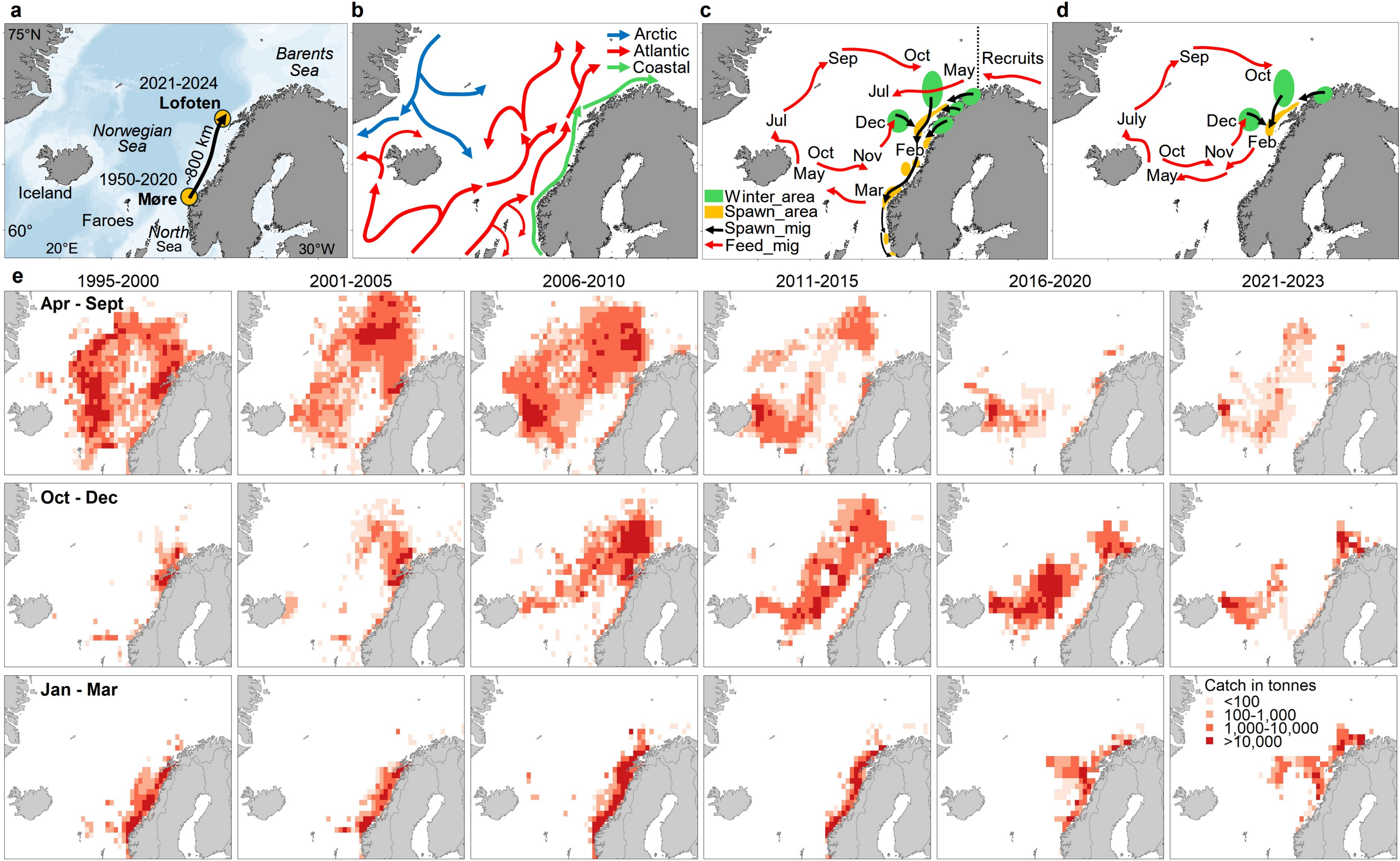
a
75°N
Barents Sea
2021-2024
Lofoten
Norwegian Sea
~800 km
1950-2020
Iceland
Møre
Faroes
60°
North Sea
20°E
30°W
b
Arctic
Atlantic
Coastal
c
Sep
Oct
May
Recruits
Jul
Jul
Dec
Feb
Oct
Nov
May
Mar
Winter_area
Spawn_area
Spawn_mig
Feed_mig
d
Sep
Oct
July
Dec
Feb
Oct
Nov
May
e
1995-2000
2001-2005
2006-2010
2011-2015
2016-2020
2021-2023
Apr - Sept
Oct - Dec
Jan - Mar
Catch in tonnes
<100
100-1,000
1,000-10,000
>10,000

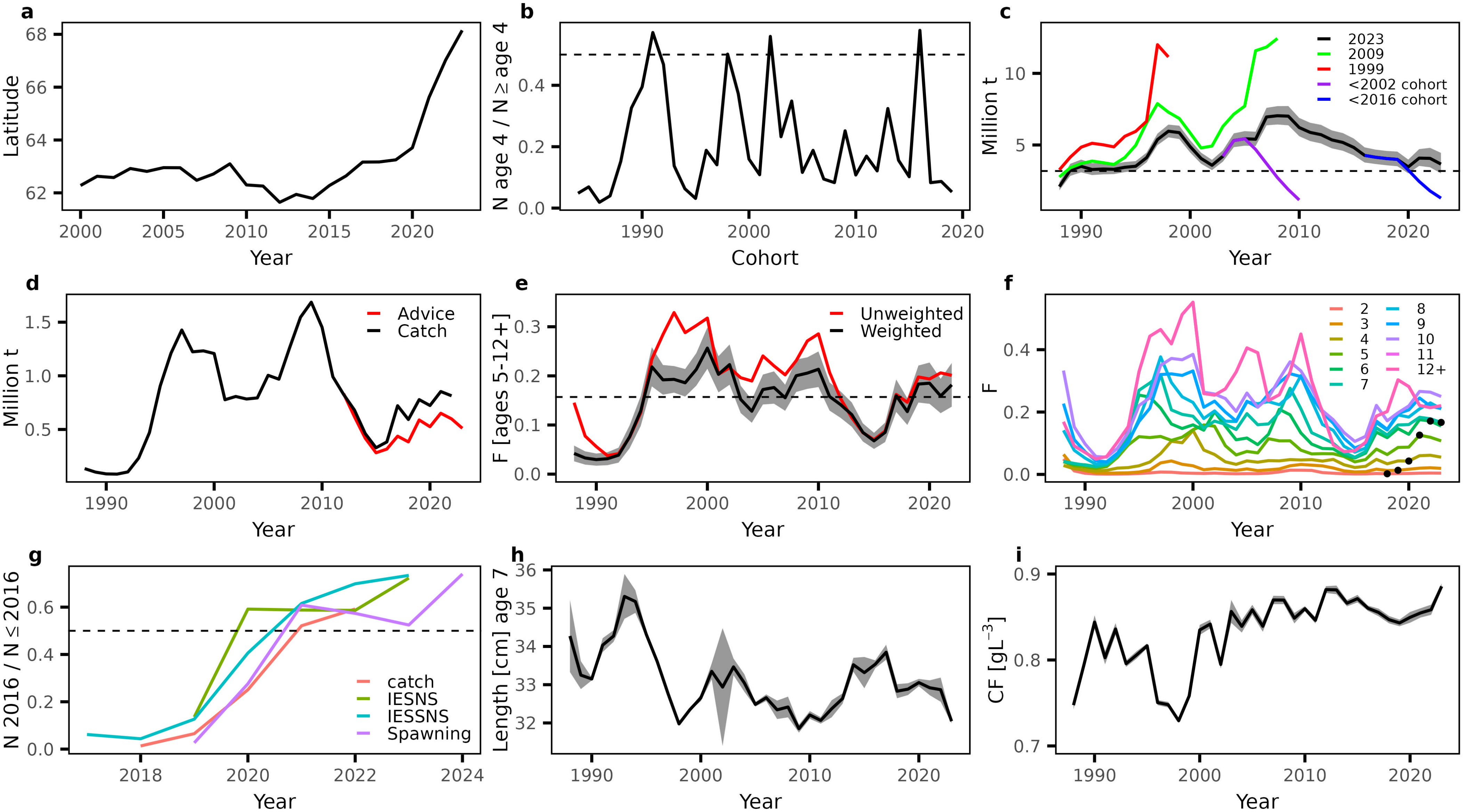
a
Latitude
62
64
66
68
2000
2005
2010
2015
2020
Year
b
N age 4 / N ≥ age 4
0.0
0.2
0.4
1990
2000
2010
2020
Cohort
c
Million t
5
10
2023
2009
1999
<2002 cohort
<2016 cohort
1990
2000
2010
2020
Year
d
Million t
0.5
1.0
1.5
Advice
Catch
1990
2000
2010
2020
Year
e
F [ages 5-12+]
0.0
0.1
0.2
0.3
Unweighted
Weighted
1990
2000
2010
2020
Year
f
F
0.0
0.2
0.4
2
3
4
5
6
7
8
9
10
11
12+
1990
2000
2010
2020
Year
g
N 2016 / N ≤ 2016
0.0
0.2
0.4
0.6
catch
IESNS
IESSNS
Spawning
2018
2020
2022
2024
Year
h
Length [cm] age 7
32
33
34
35
36
1990
2000
2010
2020
Year
i
CF [gL$^{-3}$]
0.7
0.8
0.9
1990
2000
2010
2020
Year

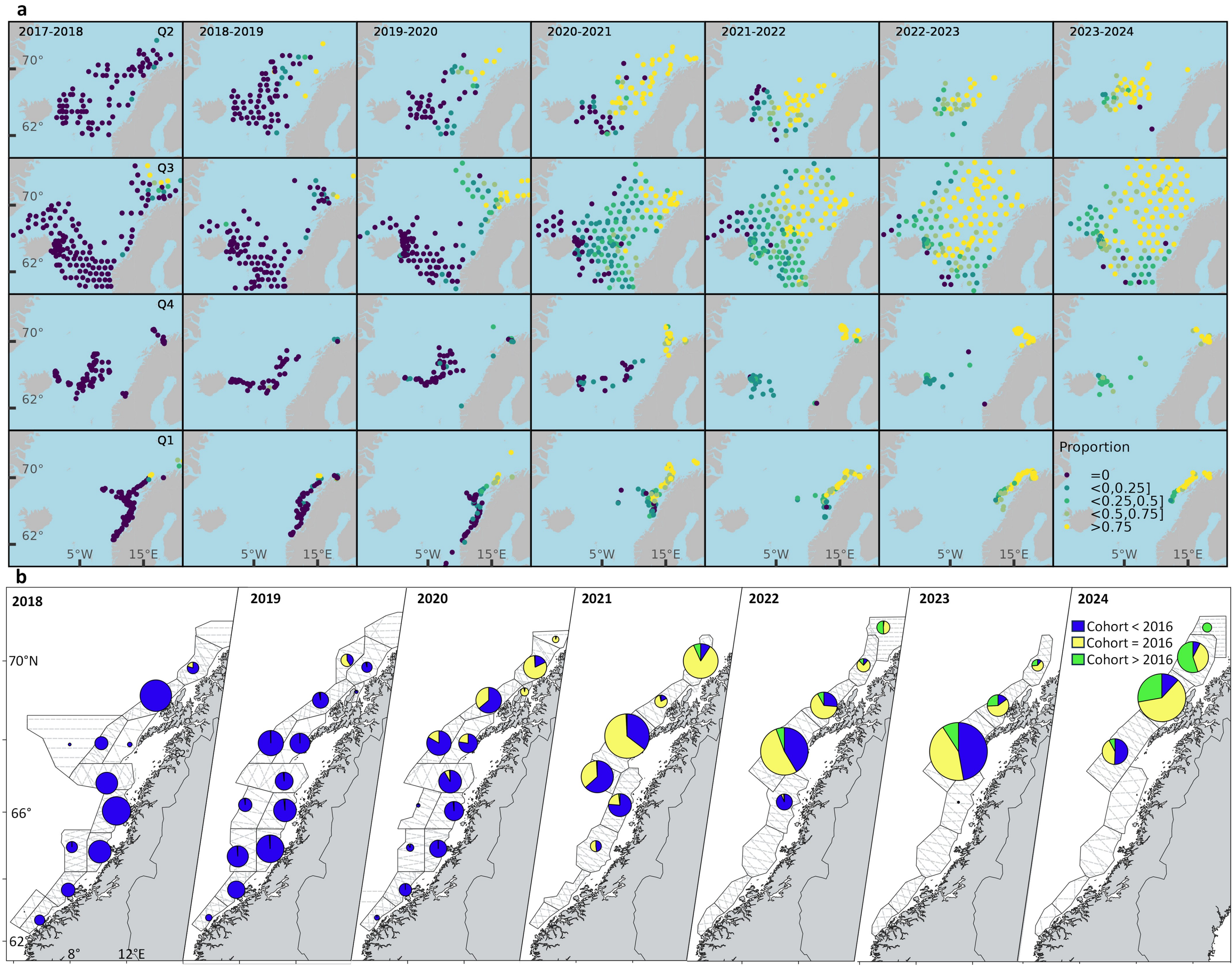
a
2017-2018
2018-2019
2019-2020
2020-2021
2021-2022
2022-2023
2023-2024
Q2
Q3
Q4
Q1
70°
62°
5°W
15°E
Proportion
=0
<0,0.25]
<0.25,0.5]
<0.5,0.75]
>0.75
b
2018
2019
2020
2021
2022
2023
2024
Cohort < 2016
Cohort = 2016
Cohort > 2016
70°N
66°
62°
8°
12°E

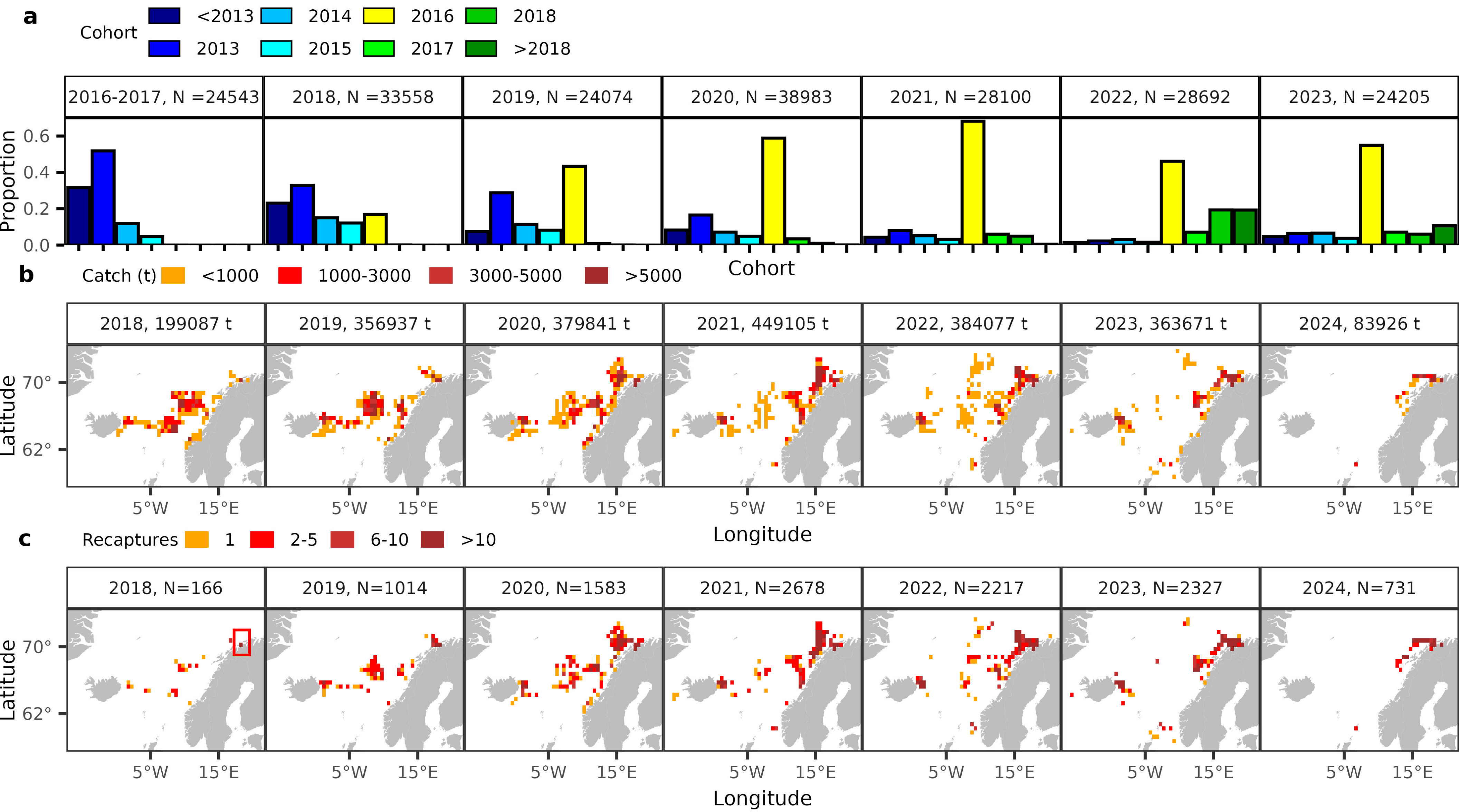
a
Cohort
<2013
2013
2014
2015
2016
2017
2018
>2018
2016-2017, N =24543
2018, N =33558
2019, N =24074
2020, N =38983
2021, N =28100
2022, N =28692
2023, N =24205
Proportion
0.0
0.2
0.4
0.6
Cohort
b
Catch (t)
<1000
1000-3000
3000-5000
>5000
2018, 199087 t
2019, 356937 t
2020, 379841 t
2021, 449105 t
2022, 384077 t
2023, 363671 t
2024, 83926 t
Latitude
70°
62°
5°W
15°E
Longitude
c
Recaptures
1
2-5
6-10
>10
2018, N=166
2019, N=1014
2020, N=1583
2021, N=2678
2022, N=2217
2023, N=2327
2024, N=731
Latitude
70°
62°
5°W
15°E
Longitude

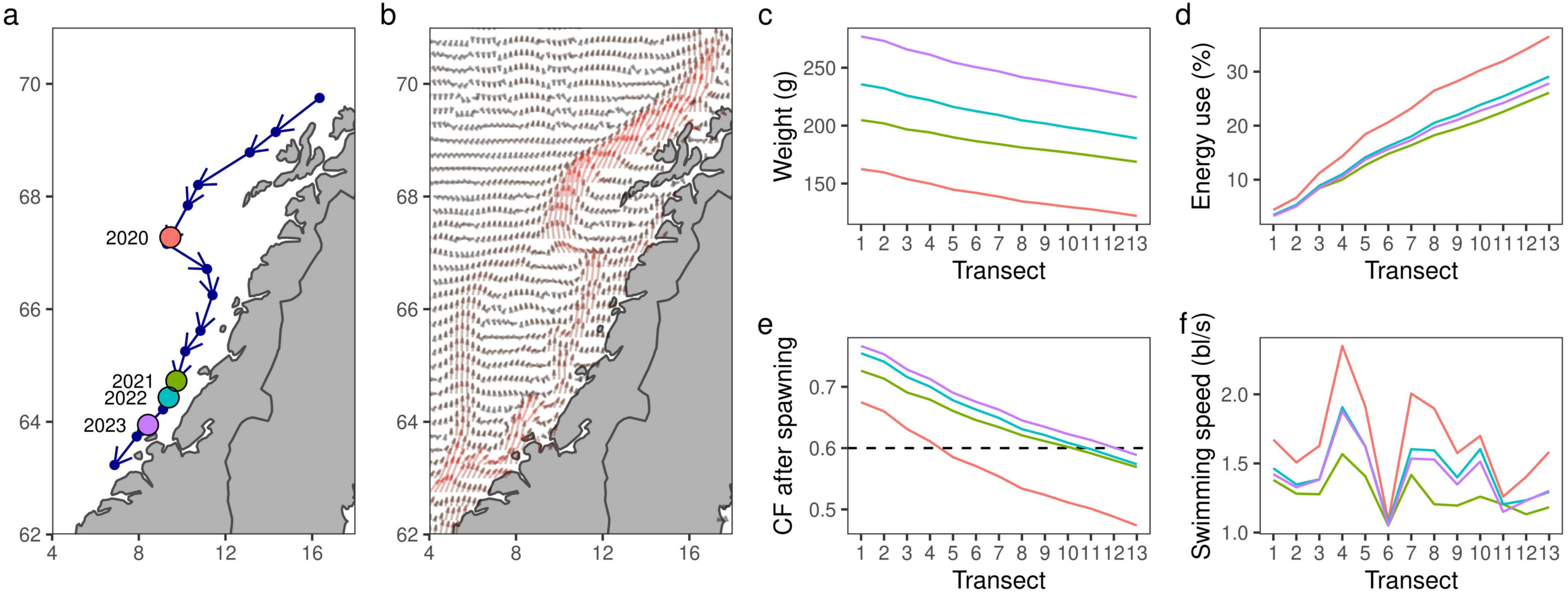
a
b
c
d
e
f
70
68
66
64
62
4
8
12
16
2020
2021
2022
2023
Weight (g)
250
200
150
Energy use (%)
30
20
10
CF after spawning
0.7
0.6
0.5
Swimming speed (bl/s)
2.0
1.5
1.0
1 2 3 4 5 6 7 8 9 10 11 12 13
Transect